

INVESTIGATION OF CHLOROPHYLL-A VARIABILITY IN RED SEA USING SATELLITE-BASED METEOROLOGY AND OCEANOGRAPHY DATA

Anton Satria PRABUWONO¹, KUNARSO^{2,3*}, Anindya WIRASATRIYA^{2,3}
Satria ANTONI^{4,5}

DOI: 10.21163/GT_2023.182.18

ABSTRACT :

The Red Sea has a special geographical feature because it is situated in the tropical and subtropical zones. The uniqueness of the Red Sea makes a variability of oceanography data (Chlorophyll-a (Chl-a), current, Salinity, etc.) and meteorological data (Precipitation, Wind Speed, etc.). However, investigations of differences interaction of oceanography and meteorology are less studied in of the Red Sea. Satellites and modeling make it possible to observe oceanographic and meteorological data over a long period of time. This study first demonstrates that there are three major areas along the Red Sea that represent the different Chl-a concentrations during the rainy season. The month of July has the highest Chl-a concentration in the south (1.3 mg/m³) and the lowest Chl-a concentration in the north (0.18 mg/m³). The southern part of the Red Sea has a different generation mechanism from the northern part of the Red Sea in terms of increasing and decreasing Chl-a concentrations. The existence of surface runoff in this area may result in the supply of anthropogenic organic compounds and fresh water to coastal waters. This may increase the supply of nutrients at the peak of the rainy season, and finally increase the concentration of Chl-a in the southern part. In the middle part, the variability of Chl-a is mainly affected by wind speed. Meanwhile, the high salinity in the northern part may limit the growth of phytoplankton and keep the Chl-a concentration low.

Key-words: *Chlorophyll-a, Precipitation, Salinity, Surface Runoff, Red Sea.*

1. INTRODUCTION

Chlorophyll-a (Chl-a) is a phytoplankton biomass indicator present in practically every aquatic habitat (Smith et al., 2005). As the top trophic level, it is crucial to the marine food chain. Chl-a is an important food for fish and other organisms in coral reef ecosystems (Smith et al., 2005; Zainuddin et al., 2017). The positive correlation between Chl-a and fish productivity can be seen from the lower of Chl-a corresponding to the lower fish catch. Smith et al. (2005), reported a significant positive relationship between the skipjack catches and the concentration of chlorophyll in the Gulf of Bone-Flores Sea. Furthermore, Hunt et al. (2021), reported that the Red Sea's fish catch potential is split into two areas, with the south having the highest potential and the north having the lowest. Chl-a variability characteristics in an area are essential in increasing fish catches. Furthermore, we also need to understand Chl-a variability to understand fisheries management.

The Red Sea is one of the most important marine economic and environmental assets in the Middle East (Daqamseh et al., 2019). The Red Sea is a semi enclosed waters, lies between the Asian and African continental shelves and has a complex bathymetry and topography. The Red Sea's

¹ Faculty of Computing and Information Technology in Rabigh, King Abdulaziz University, Jeddah 21589, Saudi Arabia; aprabuwono@kau.edu.sa

² Department of Oceanography, Faculty of Fisheries and Marine Sciences, Diponegoro University, Semarang 50275, Indonesia; anindyawirasatriya@lecturer.undip.ac.id; Correspondence: kumarso@lecturer.undip.ac.id.

³ Center for Coastal Disaster Mitigation and Rehabilitation Studies, Diponegoro University, Semarang 50275, Indonesia

⁴ Marine Geology Department, Faculty of Marine Sciences, King Abdulaziz University, Jeddah 21589, Saudi Arabia; suddin@stu.kau.edu.sa

⁵ Centre of Artificial Intelligence, University of Insan Cita Indonesia, Jakarta, Indonesia; satriaantoni@uici.ac.id

southern region has numerous islands and shallow bathymetry. In contrast, the northern and middle regions have fewer islands and deeper bathymetry (Raitsos et al., 2013). It can cause variations in oceanographic and meteorological variability (Munandar et al., 2023; Figa-Saldaña et al., 2002). This feature makes the Red Sea an essential region for many marine species, some of which are endemic (Belkin, 2009). Another essential feature of the Red Sea lies in the uniqueness of the coral reef ecosystem that survives with the highest salinity in the world [Nassar et al., 2014; Raitsos et al., 2011]. The range of salinity that coral reefs can survive is 28.7–40.4 ppt (Wilkinson, 2008), and the Red Sea has a salinity range of 36–40 ppt (Mezger et al., 2016). The Red Sea has the highest diversity of coral communities outside of the southeast Asian "coral triangle," with a 0.12 percent global coral reef ecosystem (Wilkinson, 2008; DeVantier et al., 2000). The water can influence the natural environment of phytoplankton communities (Mezger et al., 2016; Sew and Todd, 2020; Sugie et al., 2020; Redden and Rukminasari, 2008). Changes in salinity are the result of runoff from the mainland and the balance between precipitation and evaporation (Al-Najjar et al., 2007; Lee and Hong, 2019).

Precipitation is one of the most important climate variables that influence the variability of chlorophyll in marine ecosystems (Shou et al., 2022; Kim et al., 2014). Increased precipitation triggers a rise in nutrient supply (NO_3^-), which plays an essential role in the increase of Chl-a in coastal waters (Baker et al., 2007; Maslukah et al., 2019). Meanwhile, the variability of chlorophyll-a in offshore areas is more dominated by upwelling, downwelling, and vertical mixing caused by wind speed variability (Munandar et al., 2023; Wirasatriya et al., 2019; Siswanto et al., 2020; DeCarlo et al., 2021). The mechanisms of upwelling, downwelling, and vertical mixing can be triggered by Ekman transport, Ekman pumping, cyclonic and anticyclonic eddy, etc. (Wang and Tang, 2014). These mechanisms influence the movement of nutrients from the deep ocean to the surface and from the surface to the deep ocean (Munandar et al., 2023; Wirasatriya et al., 2019; Wirasatriya et al., 2020). The variability of nutrients in surface water can influence the growth of phytoplankton (Maslukah et al., 2019). Consequently, it is necessary to determine to what extent these parameters affect the variability of Chl-a as a representative of phytoplankton in these waters.

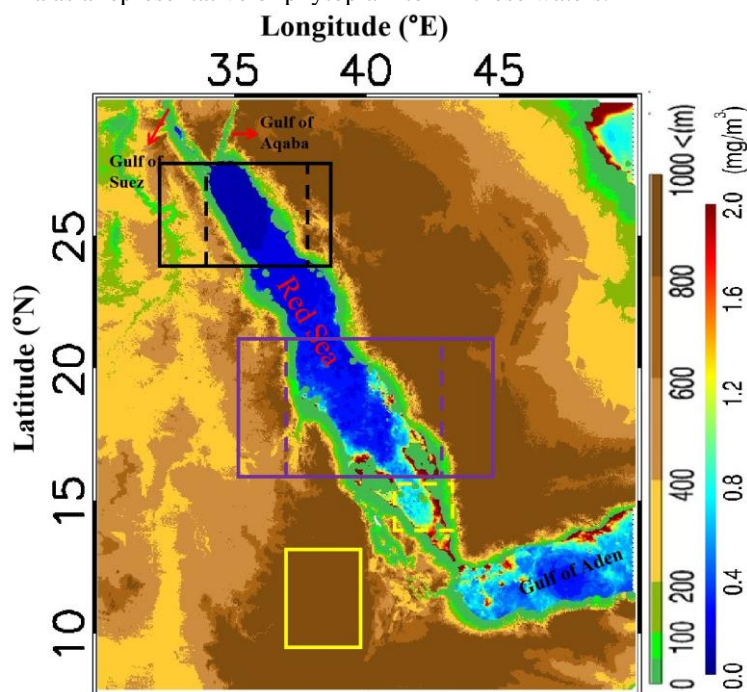


Fig. 1. Location area research with topography and Chl-a in Summer (July). Sampling areas for time series analysis (Fig. 3, 4) are denoted by the boxes. The yellow, purple and black boxes (dotted line) represent the region of the southern, middle and northern Red Sea with the highest, medium and lowest Chl-a concentration, respectively. The area for extracting the value of surface runoff and precipitation are extended into land (solid line).

Therefore, we observed the seasonal variations of Chl-a concentration in the whole area along the Red Sea. In addition, data on surface wind, surface current, current curl, precipitation, and salinity are used to comprehend the mechanisms responsible for the occurrence of these phenomena. In the present study, the analysis data came from satellite and model observation for 17 years of recording (from 2003 to 2020). In Section 2.1, we explain all remote sensing and modeling data used in this research. Furthermore, all data is averaged into seasonal variations to investigate time series and spatial variations.

2. STUDY AREA

Our study area is located at the Red Sea and the area of interest was limited for the Red Sea area bordered by 30°E - 50°E and 8°N -30°N (**Fig. 1**). The Red Sea is one of the most important marine economic and environmental assets in the Middle East (Daqamseh et al., 2019). The Red Sea is a semi enclosed waters, lies between the Asian and African continental shelves and has a complex bathymetry and topography.

3. DATA AND METHODS

3.1. Data

The data used in this study are Chl-a, surface wind, surface current, current curl, surface salinity, surface runoff and precipitation with the observation period from 2003-2020. We observed the distribution of Chl-a concentrations in the Red Sea using products from a multi-satellite collaboration of the European Space Agency (ESA) and the National Aeronautics and Space Administration (NASA). This collaboration resulted in a more accurate product, the Ocean Color-Climate Change Initiative (OC-CCI) (<http://marine.copernicus.eu/>). To create this data, the OC-CCI product used a multi-ocean-color satellite platform that included the Sea-viewing Wide Field-of-View Sensor (SeaWiFS GAC+LAC), the Medium Resolution Imaging Spectrometer (MERIS), the Moderate Resolution Imaging Spectro-radiometer (MODIS-A), and the Visible Infrared Imaging Radiometer Suite (VIIRS) (Sathyendranath et al., 2019). All satellite platforms are combined using the space-time interpolation method (Wirasatriya et al., 2019). This product has a spatial resolution of 4 km.

For investigating the surface current, we used the ocean physics reanalysis data distributed through the Copernicus Marine Environment Monitoring Service (CMEMS), i.e., GLOBAL-REANALYSIS-PHY-001-030

(https://data.marine.copernicus.eu/product/GLOBAL_MULTIYEAR_PHY_001_030/description). The grid interval of this dataset is $0.083^\circ \times 0.083^\circ$ (Drévilion et al., 2022). From surface ocean current, we calculated surface ocean curl to represent the existence of eddies.

The Advanced Scatterometer (ASCAT) is produced by the European Organization for the Exploitation of Meteorological Satellites (EUMETSAT) and has more accuracy for coastal waters compared to other products (Figa-Saldaña et al., 2002). ASCAT is a semi-daily surface wind product with a resolution of 14 km (<http://marine.copernicus.eu/>).

The precipitation data product from ERA-5 reanalysis is widely used for hydrological monitoring (<https://cds.climate.copernicus.eu/cdsapp#!/dataset/reanalysis-era5-single-levels?tab=form>). ERA5 precipitation data is generated using a combination of modelling and data assimilation systems (Lavers et al., 2022). ERA5 output is provided hourly, and the resolution of this dataset is 30 km. Data on sea surface salinity were obtained from Remote Sensing Systems' Soil Moisture Active Passive (SMAP) version 2.0 (<https://www.remss.com/missions/smap/salinity/>). The resolution of SMAP 2.0 is 70 km, but the 70 km product is resampled into 0.25° . The accuracy product, SMAP 2.0, is higher if compared with SMAP 1.0 (AlJassar et al., 2022).

The surface runoff data is obtained from ERA5 data which is the fifth generation European Centre for Medium-Range Weather Forecasts (ECMWF) reanalysis for the global climate and weather for the past 8 decades. This is hourly data with grid interval of $0.25^\circ \times 0.25^\circ$ (<https://cds.climate.copernicus.eu/cdsapp#!/dataset/reanalysis-era5-single-levels?tab=overview>).

3.2. Method

The data in this study were collected over various time periods of observation (hourly, semi-daily, daily, and monthly), so all data needs to be averaged into monthly climatological data to facilitate analysis. To composite the data, we used the formula described in (Wirasatriya et al., 2017).

$$\bar{X}(a, b) = \frac{i}{m} \sum_{i=1}^m x_i(a, b, t) \quad (1)$$

where (a, b) is the monthly climatology at a, b , and $x_i(a, b, t)$ is the i -th data value at position a (longitude), b (latitude), and t (time). Furthermore, m is the number of time periods of observation for the monthly climatology calculation. Additionally, the Not a Number (NaN) data is excluded from the calculation of the monthly climatology calculation.

We analyzed the spatial distribution of all data by season i.e. winter, spring, summer and autumn as represented by January, April, July, and October, respectively.

To investigated the influence of eddies forcing on chlorophyll-a in the Red Sea, we convert surface current data into *current curl* (Wang and Tang, 2014):

$$\text{Current Curl} = \frac{\partial V}{\partial x} - \frac{\partial U}{\partial y} \quad (2)$$

where V is wind stress from meridional component and U is wind stress from zonal component.

4. RESULTS AND DISCUSSIONS

4.1. Spatial Distribution of Chl-a, Current Curl, Surface Current, and Surface Wind

The results of the spatial distribution of the monthly climatology of Chl-a in the Red Sea in January, April, July, and October (**Fig. 2**) and the Chl-a concentration detected appear in three areas (**Fig. 1**). The three locations studied have low (northern part), medium (middle part), and high (southern part) Chl-a concentrations, respectively. In the northern part, Chl-a concentrations reach 0.18 mg/m^3 in October and 0.28 mg/m^3 in February (**Fig. 3**). In the middle part, Chl-a concentrations reach 0.4 mg/m^3 in April and 0.8 mg/m^3 in July (**Fig. 3**). In the southern part, Chl-a concentrations reach 0.5 mg/m^3 in May and 1.3 mg/m^3 in July (**Fig. 3**). The difference in Chl-a concentration in the Red Sea is clearly seen, and it is indicated that the Red Sea has different mechanisms to generate increases and decreases in Chl-a concentration. The variability of the Chl-a concentration in the on-shore and off-shore areas can be triggered by wind, current, tide, run-off from the mainland, etc. (Munandar et al., 2023; Kim et al., 2014; Wirasatriya et al., 2020; Wang and Tang, 2014).

To investigate the Chl-a variability mechanisms, we examined the relation between Chl-a and surface wind. In the southern part, surface winds reached 5.5 m/s (November) and 1 m/s (May), surface winds in the middle part reached 3.5 m/s (July) and 1.5 m/s (October), and in the northern part, surface winds reached 4.25 m/s (June and September) and 3.25 m/s (April) (**Fig. 3**). Previous studies found that strong surface winds mostly influence the increasing Chl-a (Wirasatriya et al., 2019; Iwasaki, 2020; Liu et al., 2020). In the middle part, the relationship between surface wind and Chl-a has the same pattern. It is indicated that surface wind can generate vertical mixing and become the primary process for increasing Chl-a in the middle part of the Red Sea. However, we found an inconsistent relationship between wind speed and Chl-a in the southern and northern parts of the Red Sea. The variability of Chl-a does not follow the variation of surface wind. In the southern part, the increasing surface wind increases Chl-a a little from the previous month (September–October) from 0.8 to 1 mg/m^3 , but not higher than July (1.3 mg/m^3). In the northern part, the strong wind speed does not influence the increase of Chl-a. Munandar et al. (2023) found that in the Sulu Sea, surface wind is not the primary data to trigger high Chl-a, but tide is the primary process to trigger high Chl-a. Thus, surface wind in the northern and southern parts of the Red Sea has less influence on the variability of Chl-a in the Red Sea and indicates a different mechanism for the variability of Chl-a in the Red Sea.

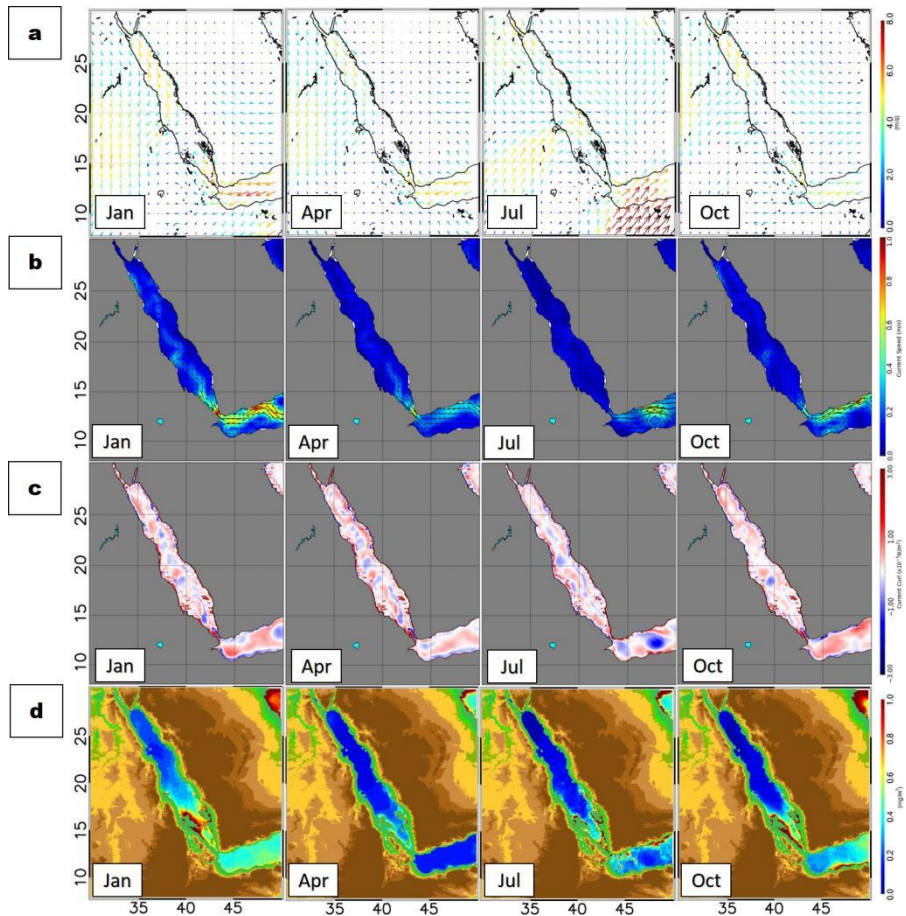


Fig. 2. The spatial distribution of the monthly climatology of (a) Surface wind, (b) Surface current, and (c) Curl current and (d) Chl-a along the Red Sea in January, April, July and October (2003–2020).

We also investigate the relation between Chl-a and current speed, the current speed is high in the southern part (0.6 m/s) in January and lower on the other. Raitso et al. (2013) indicate that the existence of cyclonic and anticyclonic eddies along the Red Sea contributes to the variability of Chl-a. To represent the variability of eddy, we convert current speed to current curl, and compare it to Chl-a (**Fig. 2 c, d**). The existence of cyclonic and anticyclonic eddies along the Red Sea is indicated by positive and negative curl, respectively. The distribution of surface current and current curl do not show that there are strong cyclonic and anticyclonic eddies in the Red Sea. Interestingly, the cyclonic and anticyclonic eddies are stronger in the Gulf of Aden (southern part of the Red Sea). In the Gulf of Aden, strong anticyclonic eddies occur in July and cause Chl-a decrease. Furthermore, cyclonic eddies detected in October, and their occurrences increases Chl-a. In contrast, the curl pattern in the Red Sea as not as clear as the Gulf of Aden. Thus, eddy currents are not the primary processes that trigger increasing Chl-a in the Red Sea but the play important role to distribute Chl-a in the Red Sea as mentioned by Raitso et al. (2013). This indicates a different mechanism for the generating factor of increasing Chl-a in the Red Sea.

4.2. Time Series investigation of Chl-a, Surface Wind, and Precipitation

The previous analysis found that surface wind and current do not play a significant role in chlorophyll variability in the northern and southern parts of the Red Sea. We investigated the time series variability of precipitation and Chl-a to investigate the inconsistency of the relationship

between wind speed and Chl-a in the southern Red Sea. Kim et al. (2014) and Wirasatriya et al. (2021) found that precipitation plays an important role in increasing Chl-a in the on-shore area. The precipitation extraction area was expanded in order to observe mainland runoff in the southern Red Sea (Figure 1). In the southern part, the intensity of precipitation is 14–30 times higher (14 mm/day) than precipitation in the northern and middle areas (Fig. 3). Higher precipitation in the southern part occurs in July, at the same time as the peak of Chl-a concentration (1.3 mg/m³). Precipitation can influence the variability of Chl-a in on-shore areas because, during the rainy season, it can change the amount of nutrients coming from runoff on the mainland. Increased runoff water from the mainland has an impact on the nutrients (phosphate, nitrate, etc.) in coastal waters and becomes an important material for phytoplankton to conduct photosynthesis (Baker et al., 2007; Maslukah et al., 2019; Gittings et al., 2018).

To investigate the evidence of high runoff from land during high rainfall, we analyzed surface runoff in the southern part of the Red Sea. The peak of surface runoff reached $150 \times 10^3 \text{ m}^3/\text{s}$ in July and decreased in the next month. It has the same pattern with precipitation and Chl-a in the southern part. The influx of mainland runoff is characterized by an increase in surface runoff in July, as well as the occurrence of Chl-a and precipitation peaks (Fig. 4). This indicates that precipitation is the primary process contributing to the variability of Chl-a in the southern part of the Red Sea.

Nevertheless, the precipitation in the northern part reaches only 0,18 mm/day, which is lower than in other parts. This reinforces the fact that wind speed and precipitation are not the primary processes that trigger the variability of Chl-a in this area. This indicates another factor influences the occurrence of variability in Chl-a concentration in the northern part of the Red Sea.

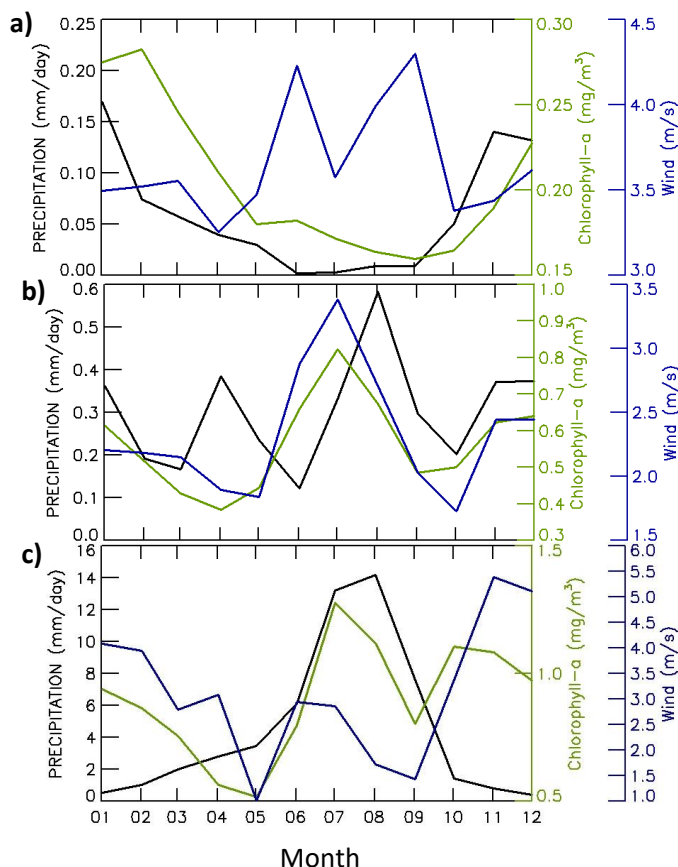


Fig. 3. Time series data of the monthly climatology of Chl-a, surface wind speed, and precipitation in three areas (a= northern, b= middle, c= southern).

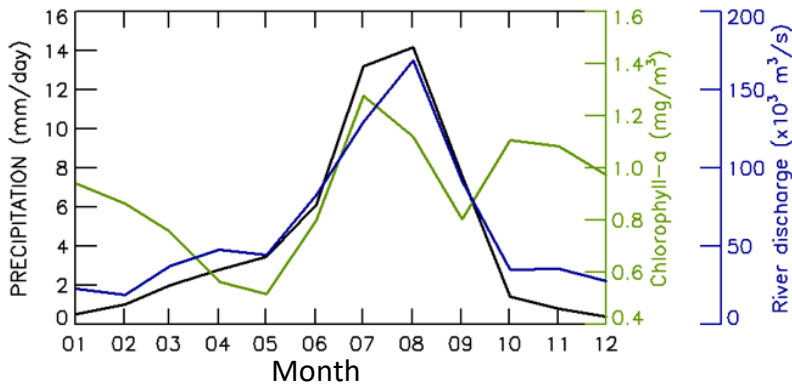


Fig. 4. Time series data of Chl-a, surface runoff, and precipitation in the southern part of Red Sea.

4.3. Time Series investigation of Chl-a, Surface Wind, and Salinity

In the northern part of the Red Sea the variability of Chl-a does not match with the wind speed and precipitation (**Fig. 3a**). In this area, the wind speed increases between the May - September reach 3.4 – 4.4 m/s and precipitation increase between the November - January reach 0.05 – 0.18 mm/day. Wind speed values in the northern is not lower than other areas, but the value of Chl-a in the northern is lower compared to other areas.

As shown earlier, Chl-a in the north was lower than in other areas and this could be because the northern part has higher salinity. Moreover, the northern part is included in the sub-tropical region. To investigate more about this phenomenon, we analyze the meridional propagation of salinity, Chl-a and surface wind along the Red Sea. We took 14 sample areas in $0.5^\circ \times 0.5^\circ$ bins and the plot the monthly climatology of salinity, Chl-a and surface wind speed in Hovmöller diagram as shown in **Fig. 5**. In the middle and southern parts, the salinity reaches 35-38 ppt and in the north it reaches >38.5 ppt. the high salinity in the northern area may become the limiting factor for several organisms including phytoplankton in the sea to survive and grow. Ismael (2015) reported a gradual decrease in phytoplankton richness from the southern Red Sea to the Gulf of Suez.

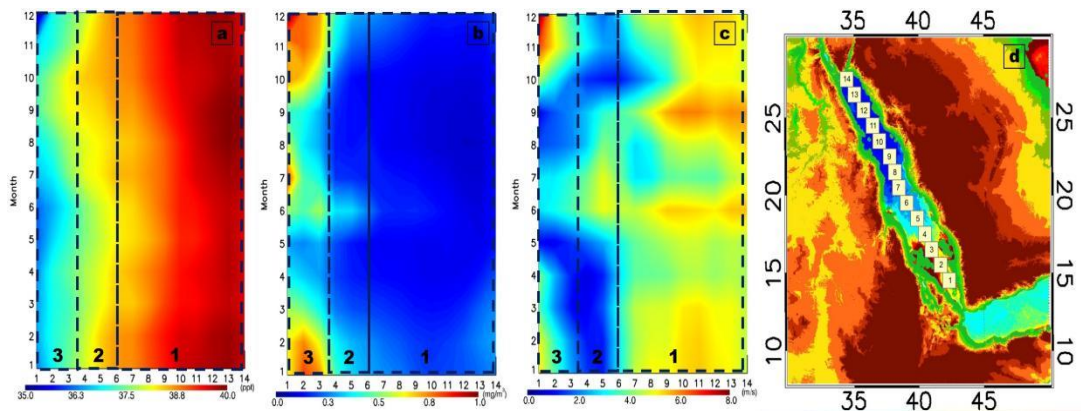


Fig. 5. Hovmöller diagram of monthly climatology of (a) salinity, (b) Chl-a, and (c) surface wind (C) with bin number at x-axis. The bins with numbers used for creating Hovmöller are shown in (d). Dashed black box donates the area of observation 1 (northern), 2 (middle), 3 (southern).

The high (low) salinity impact to low (high) Chl-a.

5. DISCUSSION

According to previous research, the Red Sea is known for having high Chl-a concentrations during the winter (December-March) and low concentrations during the summer (May-September) (Raitsos et al., 2013; Raitsos et al., 2015). An essential mechanism for influencing the high Chl-a in the Red Sea found by [Raitsos et al., 2013; Gittings et al., 2021] is eddy current and vertical mixing, which supply nutrients from deeper waters. We discovered the time difference and the mechanism causing the increase and decrease of Chl-a concentration in the Red Sea. This vertical mixing may occur in winter because wind speeds are higher in the Red Sea from November to December. However, higher wind speeds are unrelated to increased Chl-a concentration (July) in the Red Sea. More clearly affecting the increase in Chl-a are salinity and precipitation in the northern and southern parts of the Red Sea, respectively. Vertical mixing is shown in the middle part of the Red Sea, even though the wind speed values are lower compared to other areas. Furthermore, the impact of wind speed in the southern affects the increase in Chl-a in October, but not higher than precipitation in July (Fig. 3c).

The climatological and meteorological analysis determine the essential factors that influence the increase in Chl-a in the Red Sea (Acker et al., 2008). As presented in this study, the southern part of the Red Sea clearly shows that precipitation can affect the variability of Chl-a caused by mainland runoff. In accordance with the result of Racault et al. (2015), the highest Chl-a occurs during summer and we found that it occurs under the condition of highest precipitation and surface runoff. As found by (Kim et al., 2014; Wirasatriya et al., 2017; Wang and Tang, 2014; Iwasaki, 2020; Kunarso et al., 2019), the increases in wind speed and precipitation greatly affect the variability of Chl-a. The mainland runoff may supply nutrients to coastal areas and can be part of the items for the photosynthesis mechanism. Therefore, this finding completes the results of Dreano et al. (2016) and Triantafyllou et al. (2014), who found the subsurface intrusion from the Gulf of Aden that plays a key role in the development of the southern Red Sea phytoplankton blooms during winter. However, the use of satellite imagery to analyze the effect of precipitation on Chl-a needs to be done carefully because the total suspended matter factor in the waters can affect the accuracy of the data. The periodic collection of field observations needs to be done to improve the accuracy of satellite imagery by creating an algorithm suitable for the Red Sea conditions. Future research is required to improve and extend this task.

The different conditions in the northern part of the Red Sea, where salinity is a limiting factor in the growth of phytoplankton. As summarized by (Mezger et al., 2016; Sew and Todd, 2020; Putland and Iverson, 2007), in areas with four seasons the salinity value suitable for the growth of phytoplankton ranges from 20-30 ppt. Sugie et al. (2020) found that waters with low to moderate salinity or in the upper reaches had higher levels of Chl-a. Furthermore, research in the laboratory conducted by Yun et al. (2019) revealed that increased salt levels in the waters affect the growth of phytoplankton. The high salinity in the northern part of the Red Sea can be affected by lower precipitation, so that the surface runoff in this area becomes less. The lower surface runoff can influence the high salinity in the water (Sew and Todd, 2020; Sugie et al., 2020; Redden and Rukminasari, 2008; Fisher et al., 1988), respectively. However, a more thorough analysis is needed regarding the types of phytoplankton that live in the Red Sea because some phytoplankton have different salinity tolerances. Future research is required to improve and extend this task.

6. CONCLUSIONS

Utilizing satellite observations, Chl-a variability in the Red Sea is characterized by highest, medium and lowest concentration in the southern, middle, and northern parts, respectively. In the southern part, the highest Chl-a (i.e., 1.3 mg/m³) occurs during summer as a result of high precipitation that may bring nutrient from land via surface runoff. In the middle part, the highest Chl-a (i.e., 0.8 mg/m³) also occurs during summer. However, wind speed play more important role to control the variability of Chl-a than precipitation. In the northern part, the Chl-a concentration is very low, even during the peak in winter, the concentration is only 0.28 mg/m³. The high salinity (> 38.5 ppt) in the northern part may become the limiting factor for phytoplankton to survive and grow.

ACKNOWLEDGMENTS

We are thankful for the data provided by NASA, ESA, EUMETSAT, and other stakeholders for this article. This research was funded by Institutional Fund Projects under grant no. (IFPIP:1424-830,1442). Therefore, authors gratefully acknowledge technical and financial support from the Ministry of Education and King Abdulaziz University, DSR, Jeddah, Saudi Arabia. Thanks to Bayu Munandar and Ardiansyah Desmont Puryajati for their contributions to this article.

REFERENCES

- Acker, J., Leptoukh, G., Shen, S., Zhu, T., & Kempler, S. (2008). Remotely-sensed chlorophyll a observations of the northern Red Sea indicate seasonal variability and influence of coastal reefs. *Journal of Marine Systems*, 69, 191-204. <https://doi.org/10.1016/j.jmarsys.2005.12.006>.
- AlJassar, H., Temimi, M., Abdelkader, M., Petrov, P., Kokkalis, P., AlSarraf, H., Roshni, N., & Al Hendi, H. (2022). Validation of NASA SMAP Satellite Soil Moisture Products over the Desert of Kuwait. *Remote Sensing*, 14, 3328. <https://doi.org/10.3390/rs14143328>.
- Al-Najjar, T., Badran, M. I., Richter, C., Meyerhoefer, M., & Sommer, U. (2007). Seasonal dynamics of phytoplankton in the Gulf of Aqaba, Red Sea. *Hydrobiologia*, 579, 69–83. <https://doi.org/10.1007/s10750-006-0365-z>.
- Baker, A. R., Weston, K., Kelly, S. D., Voss, M., Streu, P., & Cape, J. N. (2007). Dry and wet deposition of nutrients from the tropical Atlantic atmosphere: Links to primary productivity and nitrogen fixation. *Deep Sea Res. Part I*, 54, 1704–1720. <https://doi.org/10.1016/j.dsr.2007.07.001>.
- Belkin, I. M. (2009). Rapid warming of large marine ecosystems. *Progress in Oceanography*, 81, 207–213. <https://doi.org/10.1016/j.pocean.2009.04.011>.
- Daqamseh, S. T., Al-Fugara, A., Pradhan, B., Al-Oraiqat, A., & Habib, M. (2019). MODIS Derived Sea Surface Salinity, Temperature, and Chlorophyll-a Data for Potential Fish Zone Mapping: West Red Sea Coastal Areas, Saudi Arabia. *Sensors*, 19, 2069. <https://doi.org/10.3390/s19092069>.
- DeCarlo, T. M., Carvalho, S., Gajdzik, L., Hardenstine, R. S., Tanabe, L. K., Villalobos, R., & Berumen, M. L. (2021). Patterns, Drivers, and Ecological Implications of Upwelling in Coral Reef Habitats of the Southern Red Sea. *Journal of Geophysical Research: Oceans*, 126, e2020JC016493. <https://doi.org/10.1029/2020JC016493>.
- DeVantier, L., Turak, E., Al-Shaikh, K., & De'ath, G. (2000). Coral communities of the central-northern Saudi Arabian Red Sea. *Fauna of Arabia*, 18, 23–66.
- Dreano, D., Raitos, D.E., Gittings, J., Krokos, G., & Hoteit, I. (2016). The Gulf of Aden Intermediate Water Intrusion Regulates the Southern Red Sea Summer Phytoplankton Blooms. *PLoS One*, 11, 1–20. <https://doi.org/10.1371/journal.pone.0168440>.
- Drévilion, M., Fernandez, E., & Lellouche, J. M. (2022). Copernicus Marine Service PUM for GLOBAL_MULTIYEAR_PHY_001_030 (<https://catalogue.marine.copernicus.eu/documents/PUM/CMEMS-GLO-PUM-001-030.pdf>).
- Figa-Saldaña, J., Wilson, J. J. W., Attema, E., Gelsthorpe, R. V., Drinkwater, M. R., & Stoffelen, A. (2002). The Advanced Scatterometer (ASCAT) on the Meteorological Operational (MetOp) Platform: A Follow on for European Wind Scatterometers. *Canadian Journal of Remote Sensing*, 28, 404–412. <https://doi.org/10.5589/m02-035>.
- Fisher, T. R., Harding Jr., L. W., Stanley, D. W., & Ward, L. G. (1988). Phytoplankton, nutrients, and turbidity in the Chesapeake, Delaware, and Hudson estuaries. *Estuarine Coastal and Shelf Science*, 27, 61–93. [https://doi.org/10.1016/0272-7714\(88\)90032-7](https://doi.org/10.1016/0272-7714(88)90032-7).
- Gittings, J. A., Raitos, D. E., Krokos, G., & Hoteit, I. (2018). Impacts of warming on phytoplankton abundance and phenology in a typical tropical marine ecosystem. *Scientific Reports*, 8, 2240. <https://doi.org/10.1038/s41598-018-20560-5>.
- Gittings, J. A., Raitos, D. E., Brewin, R. J. W., & Hoteit, I. (2021). Links between Phenology of Large Phytoplankton and Fisheries in the Northern and Central Red Sea. *Remote Sensing*, 13, 231. <https://doi.org/10.3390/rs13020231>.
- Hunt, B. P. V., Espinasse, B., Pakhomov, E. A., Cherel, Y., Cotte, C., Delegrange, A., & Henschke N. (2021). Pelagic food web structure in high nutrient low chlorophyll (HNLC) and naturally iron fertilized waters in

- the Kerguelen Islands region, Southern Ocean. *Journal of Marine Systems*, 224, 103625. <https://doi.org/10.1016/j.jmarsys.2021.103625>.
- Ismael, A. A. (2015). Phytoplankton of the Red Sea: In: Rasul, N., Stewart, I. (eds) *The Red Sea*. Springer Earth System Sciences. Springer, Berlin, Heidelberg. https://doi.org/10.1007/978-3-662-45201-1_32.
- Iwasaki, S. (2020). Daily Variation of Chlorophyll-A Concentration Increased by Typhoon Activity. *Remote Sensing*, 12, 1259. <https://doi.org/10.3390/rs12081259>.
- Kim, T., Najjar, R. G., & Lee, K. (2014). Influence of Precipitation Events on Phytoplankton Biomass in Coastal Waters of the Eastern United States. *Global Biogeochemical Cycles*, 28, 1–13. <https://doi.org/10.1002/2013GB004712>.
- Kunarso, Wirasatriya, A., Irwani, Satriadi, A., Helmi, M., Prayogi, H., & Munandar, B. (2019). Impact of Climate Variability to Aquatic Variability and Fisheries Resources in Jepara Waters. In Proceedings of 4th International Conference on Tropical and Coastal Region Eco Development. *IOP Conference Series: Earth and Environmental Science, Semarang, Indonesia*. 30-31 October 2018, 246, 012021. <https://doi.org/10.1088/1755-1315/246/1/012021>.
- Lavers, D. A., Simmons, A., Vamborg, F., & Rodwell, M. J. (2022). An evaluation of ERA5 precipitation for climate monitoring. *Quarterly Journal of the Royal Meteorological Society*, 148, 3071-3427. <https://doi.org/10.1002/qj.4351>.
- Lee, E., & Hong, S. -Y. (2019). Impact of the Sea Surface Salinity on Simulated Precipitation in a Global Numerical Weather Prediction Model. *Journal of Geophysical Research: Atmospheres*, 124, 441-1193. <https://doi.org/10.1029/2018JD029591>.
- Liu, Y., Tang, D., Tang, S., Morozov, E., Liang, W., & Sui, Y. (2020). A case study of Chlorophyll a response to tropical cyclone Wind Pump considering Kuroshio invasion and air-sea heat exchange. *Science of the Total Environment*, 741, 140290. <https://doi.org/10.1016/j.scitotenv.2020.140290>.
- Maslukah, L., Zainuri, M., Wirasatriya, A., & Salma, U. (2019). Spatial Distribution of Chlorophyll-a and Its Relationship with Dissolved Inorganic Phosphate Influenced by Rivers in the North Coast of Java. *Journal of Ecological Engineering*, 20, 18–25. <https://doi.org/10.12911/22998993/108700>.
- Mezger, E. M., de Nooijer, L. J., Boer, W., Brummer, G. J. A., & Reichart, G. J. (2016). Salinity controls on Na incorporation in Red Sea planktonic foraminifera. *Paleoceanography and Paleoclimatology*, 31, 1562-1582. <https://doi.org/10.1002/2016PA003052>.
- Munandar, B., Wirasatriya, A., Sugianto, D. N., Susanto, R. D., Purwandana, A., & Kunarso. (2023). Distinct mechanisms of Chlorophyll-a blooms occur in the Northern Maluku Sea and Sulu Sill revealed by satellite data. *Dynamics of Atmospheres and Oceans*, 102, 101360. <https://doi.org/10.1016/j.dynatmoce.2023.101360>.
- Nassar, M. Z., Mohamed, H. R., Khiray, H. M., & Rashedy, S. H. (2014). Seasonal fluctuations of phytoplankton community and physico-chemical parameters of the north western part of the Red Sea, Egypt. *Egyptian Journal of Aquatic Research*, 40, 395–403. <http://dx.doi.org/10.1016/j.ejar.2014.11.002>.
- Putland, J. N., & Iverson, R. L. (2007). Phytoplankton Biomass in a Subtropical Estuary: Distribution, Size Composition, and Carbon: Chlorophyll Ratios. *Estuaries and Coasts*, 30, 878–885. <https://doi.org/10.1007/BF02841341>.
- Raitsos, D. E., Hoteit, I., Prihartato, P. K., Chronis, T., Triantafyllou, G., & Abualnaja, Y. (2011). Abrupt warming of the Red Sea. *Geophysical Research Letters*, 38, L14601. <https://doi.org/10.1029/2011GL047984>.
- Raitsos, D. E., Pradhan, Y., Brewin, R. J. W., Stenchikov, G., & Hoteit, I. (2013). Remote Sensing the Phytoplankton Seasonal Succession of the Red Sea. *PLoS ONE*, 8, e64909. <https://doi.org/10.1371/journal.pone.0064909>.
- Raitsos, D. E., Yi, X., Platt, T., Racault, M. F., Brewin, R. J. W., Pradhan, Y., Papadopoulos, V. P., Sathyendranath, S., & Hoteit, I. (2015). Monsoon oscillations regulate fertility of the Red Sea. *Geophysical Research Letters*, 42, 855–862. <https://doi.org/10.1002/2014GL062882>.
- Racault, M. F., Raitsos, D. E., Berumen, M. L., Brewin, R. J. W., Platta, T., Sathyendranath, S., & Hoteit, I. (2015). Phytoplankton phenology indices in coral reef ecosystems: Application to ocean-color observations in the Red Sea. *Remote Sensing of Environment*, 160, 222-234. <http://dx.doi.org/10.1016/j.rse.2015.01.019>.
- Redden, A. M., & Rukminasari, N. (2008). Effects of increases in salinity on phytoplankton in the Broadwater of the Myall Lakes, NSW, Australia. *Hydrobiologia*, 608, 87–97. <https://doi.org/10.1007/s10750-008-9376-2>.

- Sathyendranath, S., Brewin, R. J. W., Brockmann, C., Brotas, V., Calton, B., Chuprin, A., Cipollini, P., Couto, A. B., Dingle, J., Doerffer, R., Donlon, C., Dowell, M., Farman, A., Grant, M., Groom, S., Horseman, A., Jackson, T., Krasemann, H., Lavender, S., Martinez-Vicente, V., Mazeran, C., Mélin, F., Moore, T. S., Müller, D., Regner, P., Roy, S., Steele, C. J., Steinmetz, F., Swinton, J., Taberner, M., Thompson, A., Valente, A., Zühlke, M., Brando, V. E., Feng, H., Feldman, G., Franz, B. A., Frouin, R., Gould Jr, R. W., Hooker, S. B., Kahru, M., Kratzer, S., Mitchell, B. G., Muller-Karger, F. E., Sosik, H. M. Voss, K. J., Werdell, J., & Platt, T. (2019). An Ocean-Colour Time Series for Use in Climate Studies: The Experience of the Ocean-Colour Climate Change Initiative (OC-CCI). *Sensors*, 19, 4285. <https://doi.org/10.3390/s19194285>.
- Sew, G., & Todd, P. (2020). Effects of Salinity and Suspended Solids on Tropical Phytoplankton Mesocosm Communities. *Tropical Conservation Science*, 13, 1–11. <https://doi.org/10.1177/1940082920939760>.
- Shou, C. –Y., Tian, Y., Zhou, B., Fu, X. –J., Zhu, Y. –J., & Yue, F. –J. (2022). The Effect of Rainfall on Aquatic Nitrogen and Phosphorus in a Semi-Humid Area Catchment, Northern China. *International Journal of Environmental Research and Public Health*, 19, 10962. <https://doi.org/10.3390/ijerph191710962>.
- Siswanto, E., Horii, T., Iskandar, I., Gaol, J. L., Setiawan, R. Y., & Susanto, R. D. (2020). Impacts of Climate Changes on the Phytoplankton Biomass of the Indonesian Maritime Continent. *Journal of Marine Systems*, 212, 103451. <https://doi.org/10.1016/j.jmarsys.2020.103451>.
- Smith, V. H., Foster, B. L., Grover, J. P., Holt, R. D., Leibold, M. A., & deNoyelles, F. (2005). Phytoplankton species richness scales consistently from laboratory microcosms to the world's oceans. *PNAS*, 102, 4393–4396. <https://doi.org/10.1073/pnas.0500094102>.
- Sugie, K., Fujiwara, A., Nishino, A., Kameyama, S., & Harada, N. (2020). Impacts of Temperature, CO₂, and Salinity on Phytoplankton Community Composition in the Western Arctic Ocean. *Frontiers in Marine Science*, 6, 821. <https://doi.org/10.3389/fmars.2019.00821>.
- Triantafyllou, G., Yao, F., Petihakis, G., Tsiaras, K. P., Raitsos, D. E., & Hoteit, I. (2014). Exploring the Red Sea seasonal ecosystem functioning using a three-dimensional biophysical model. *Journal of Geophysical Research: Oceans*, 119, 1791–1811. <https://doi.org/10.1002/2013JC009641>.
- Wang, J. J., & Tang, D. L. (2014). Phytoplankton patchiness during spring intermonsoon in Western Coast of South China Sea. *Deep-Sea Res. II*, 101, 120–128. <https://doi.org/10.1016/j.dsr2.2013.09.020>.
- Wilkinson, C. (2008). Status of coral reefs of the world: 2008. Global Coral Reef Monitoring Network and Reef and Rainforest Research Centre, Townsville, Australia, 296 p.
- Wirasatriya, A., Setiawan, R. Y., & Subardjo, P. (2017). The Effect of ENSO on the Variability of Chlorophyll-a and Sea Surface Temperature in the Maluku Sea. *IEEE Journal of Selected Topics in Applied Earth Observations and Remote Sensing*, 10, 5513–5518. <https://doi.org/10.1109/JSTARS.2017.2745207>.
- Wirasatriya, A., Sugianto, D.N., Helmi, M., Setiawan, R. Y., & Koch, M. (2019). Distinct Characteristics of SST Variabilities in the Sulawesi Sea and the Northern Part of the Maluku Sea During the Southeast Monsoon. *IEEE Journal of Selected Topics in Applied Earth Observations and Remote Sensing*, 12, 1763 – 1770. <https://doi.org/10.1109/JSTARS.2019.2913739>.
- Wirasatriya, A., Setiawan, J. D., Sugianto, D. N., Rosyadi, I.A., Haryadi, Winarso, G., Setiawan, R. Y., & Susanto, R.D. (2020). Ekman Dynamics Variability along the Southern Coast of Java Revealed by Satellite Data. *International Journal of Remote Sensing*, 41(21), 8475–8496. <https://doi.org/10.1080/01431161.2020.1797215>.
- Wirasatriya, A., Susanto, R. D., Setiawan, J. D., Ramdani, F., Iskandar, I., Jalil, R., Puryajati, A.D., Kunarso, K., & Maslukah, L. (2021). High Chlorophyll-a Areas along the Western Coast of South Sulawesi-Indonesia during the Rainy Season Revealed by Satellite Data. *Remote Sensing*, 13, 4833. <https://doi.org/10.3390/rs13234833>.
- Yun, C. –J., Hwang, K. –O., Han, S. –S., & Ri, H. –G. (2019). The Effect of Salinity Stress on the Biofuel Production Potential of Freshwater Microalgae *Chlorella Vulgaris* YH703. *Biomass and Bioenergy*, 127, 105277. <https://doi.org/10.1016/j.biombioe.2019.105277>.
- Zainuddin, M., Farhum, A., Safruddin, S., Selamat, M. B., Sudirman, S., Nurdin, N., Syamsuddin, M., Ridwan, M., & Saitoh, S. (2017). Detection of Pelagic Habitat Hotspots for Skipjack Tuna in the Gulf of Bone-Flores Sea, Southwestern Coral Triangle Tuna, Indonesia. *PLoS One*, 12, e0185601. <https://doi.org/10.1371/journal.pone.0185601>.
-